Available online at www.sciencedirect.com
ScienceDirect
Journal of Sound and Vibration 316 (2008) 298–316
JOURNAL OF SOUND AND VIBRATION
www.elsevier.com/locate/jsvi

Exact solutions for coupled free vibrations of tapered shear-flexible thin-walled composite beams

Marcelo T. Piovan[a,b,*], Carlos P. Filipich[a,c], Víctor H. Cortínez[a,b]

[a]*Centro de Investigaciones de Mecánica Teórica y Aplicada, Universidad Tecnológica Nacional FRBB, 11 de Abril 461, B8000LMI Bahía Blanca, BA, Argentina*
[b]*Consejo Nacional de Investigaciones Científicas y Tecnológicas (CONICET), Argentina*
[c]*Departamento de Ingeniería, Universidad Nacional del Sur, Argentina*

Received 20 June 2007; received in revised form 15 February 2008; accepted 18 February 2008
Handling Editor: S. Bolton

Abstract

In this paper, analytical solutions for the free vibration analysis of tapered thin-walled laminated-composite beams with both closed and open cross-sections are developed. The present study is based on a recently developed model that incorporates in a full form the shear flexibility. The model considers shear flexibility due to bending as well as warping related to non-uniform torsion. The theory is briefly reviewed with the aim to present the equilibrium equations, the related boundary conditions and the constitutive equations. The stacking sequences in the panels of the cross-sections are selected in order to behave according to certain elastic coupling features. Typical laminations for a box-beam such as circumferentially uniform stiffness (CUS) or circumferentially asymmetric stiffness (CAS) configurations are adopted. For open cross-sections, special laminations behaving elastically like the CAS and CUS configurations of closed sections are also taken into account.

The exact values (i.e. with arbitrary precision) of frequencies are obtained by means of a generalized power series methodology. A recurrence scheme is introduced with the aim to simplify the algebraic manipulation by shrinking the number of unknown variables. A parametric analysis for different taper ratios, slenderness ratios and stacking sequences is performed. Numerical examples are also carried out focusing attention in the validation of the present theory with respect to 2D FEM computational approaches, as well as to serve as quality test and convergence test of former finite elements schemes.

1. Introduction

The increasing employment of composite materials, instead of isotropic materials, in structural components is motivated due to the evidence that composite structures have many advantages with respect to the isotropic

*Corresponding author at: Centro de Investigaciones de Mecánica Teórica y Aplicada, Universidad Tecnológica Nacional FRBB, 11 de Abril 461, B8000LMI Bahía Blanca, BA, Argentina. Tel.: +54 291 4555 220; fax: +54 291 4555 311.
E-mail addresses: mpiovan@frbb.utn.edu.ar (M.T. Piovan), cfilipich@yahoo.com.ar (C.P. Filipich), vcortine@frbb.utn.edu.ar (V.H. Cortínez).

0022-460X/$ - see front matter © 2008 Elsevier Ltd. All rights reserved.
doi:10.1016/j.jsv.2008.02.044

counterparts. The most well known features of composite materials are high strength and stiffness properties together with a low weight, good corrosion resistance, enhanced fatigue life and low thermal expansion properties among others [1]. Another interesting aspect of composite materials is the very low machining cost with respect to the common machining procedures for isotropic materials such as steel, aluminum or titanium [2]. As a result of the mentioned context, the analysis of the static and dynamic behavior of composite thin-walled beams is the subject of deep investigation. Many research activities have been devoted toward the development of theoretical and computational methods for the appropriate analysis of such members.

The first consistent study dealing with the static structural behavior of thin-walled composite-orthotropic members under various loading patterns was carried out by Bauld and Tzeng [3]. These authors employed Vlasov hypotheses in order to derive a beam theory for the analysis of fiber-reinforced members featuring open cross-sections with symmetric laminates. This theory for non-shear deformable thin-walled beam was restricted to structural members constructed with special orthotropic stacking sequences and employed only for static analysis. However, further contributions of many authors since the early eighties until the present time have made possible to extend Vlasov models by considering shear deformability due to bending, warping effects, among others. The resulting models have been employed in many problems such as free/forced vibration, elastic stability, etc.

Models for thin-walled composite beams allowing for some effects of shear deformability were already presented in the middle eighties by Giavotto et al. [4] and Bauchau [5]. In these works the effect of the warping-torsion shear deformability was not appropriately taken into. The issues related to shear deformability in composite beams were slightly studied in a few problems of static's and dynamics.

In the late eighties and the nineties a considerable number of new models and uses were developed. Some researchers [6–9] studied the non-conventional effects of constitutive elastic couplings (such as bending–bending coupling or bending–shear coupling, etc.) in the mechanics of cantilever box-beams considering only the bending component of shear flexibility whereas the warping torsion shear flexibility was neglected. However, in these models [6–9] new extensions such as the consideration of the thickness effects in shear and warping deformations, among others were introduced. Moreover, new studies devoted to the dynamical aspects of elastic couplings were performed.

Recently, Cortínez and Piovan [10] employed the Hellinger–Reissner principle to derive a theory of thin-walled beams with symmetric balanced laminates, in which the full shear flexibility was considered. This model covered topics of dynamics under states of initial normal stresses, also accounting for in-thickness shear flexibility and warping.

Many of the aforementioned models were employed for eigenvalue calculation, among other problems. However, in those numerical studies only beams with uniform cross-section were considered. There is evidence of some works devoted to the free vibration analysis of tapered beams with thin-walled cross-sections made of isotropic material [11] and with solid cross-section made of composite materials [12]. However, despite the importance of the vibratory problems in robotic arms and rotor-blades among other applications, there is scarce evidence [13] of studies focused in the free vibrations of thin-walled tapered beams made of composite materials with elastic coupling effects.

In the present work, a power series methodology is employed to calculate the exact (or with arbitrary precision) free vibration frequencies of composite thin-walled tapered beams allowing for shear flexibility due to bending as well as non-uniform torsion warping. Several studies for box-beams and I-beams with special lamination are carried out. The effects of taper and the elastic couplings are analyzed and their influence in the free vibration patterns of the beam structures appropriately enhanced. In order to show the accuracy and practical effectiveness of the model and present series approach, some comparisons with former finite element approaches, as well as shell finite elements of the commercial program COSMOS/M are performed.

2. Description of the model

In Fig. 1 a sketch of a thin-walled beam is shown. In this figure, it is possible to see the reference points **C** and **B**. The main reference point **C** is located at the geometric center of the cross-section, where the x-axis is parallel to the longitudinal axis of the beam, while y-axis and z-axis are the axes associated to the cross-section, but not necessarily the principal ones. The point **B** is a generic point belonging to the middle line of the

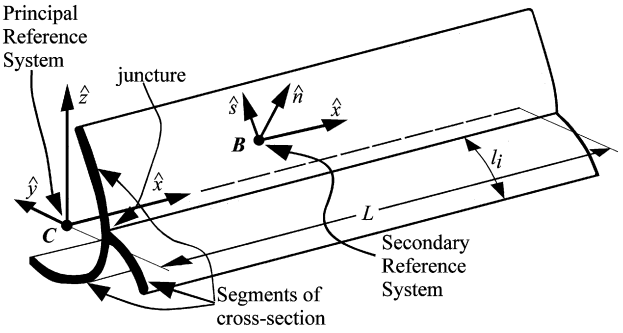

Fig. 1. Sketch of the thin-walled beam.

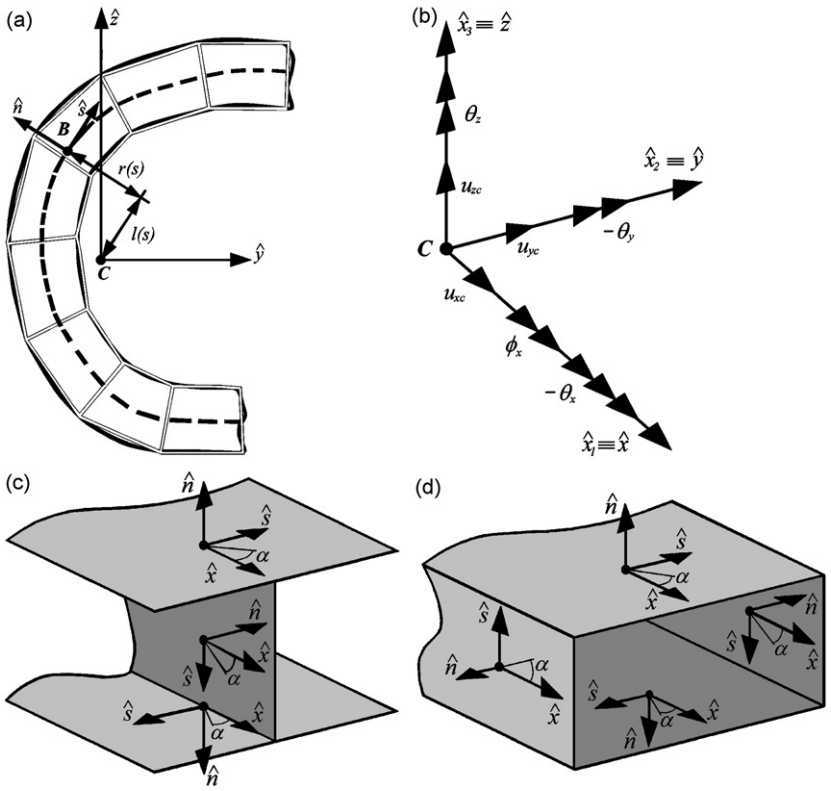

Fig. 2. (a) Description of cross-section geometrical entities and (b) displacement parameters. Secondary or lamination reference systems for the segments of open (c) and closed (d) cross-sections, respectively.

cross-sectional wall (see Fig. 2a); its co-ordinates are denoted as $Y(s)$ and $Z(s)$. The Fig. 2b shows the displacement parameters of the model. Fig. 2c and d show the reference system for each laminated segment of open and closed cross-sections, respectively.

The beam model employed in this study has been developed [10,14,17] under the following hypotheses: (a) the cross-section contour is rigid in its own plane; (b) the warping distribution is assumed to be composed by contour (or primary) and thickness (or secondary) components; (c) in the panels, the shell force and shell moment corresponding to the hoop stress σ_{ss} and the force resultant corresponding to the in-thickness stress σ_{ns} are neglected; (d) the radius of curvature at any point of the shell is neglected; (e) twisting curvature of the shell is expressed according to the classical plate theory, but bending curvature is expressed according to the first-order shear deformation theory; (f) special stacking sequences are adopted such as circumferentially

uniform stiffness (CUS) or circumferentially asymmetric stiffness (CAS) or any other lamination scheme that provides a specialized elastic coupling among twisting, bending and/or extension; (g) taking into account the comparative evidence of previous theoretical beam models [16] with experimental data and 2D–3D computational approaches, the shear flexibility due to in-thickness strains is neglected.

Under this context, the mechanics of a thin-walled beam model allowing for shear flexibility due to bending and warping can be described, in terms of beam-stress-resultants, with the following differential equations [10,14]:

$$-\frac{\partial Q_X}{\partial x}+\bar{M}_1(x)=0,\quad -\frac{\partial Q_Y}{\partial x}+\bar{M}_2(x)=0,\quad \frac{\partial M_Z}{\partial x}-Q_Y+\bar{M}_3(x)=0, \tag{1a–c}$$

$$-\frac{\partial Q_Z}{\partial x}+\bar{M}_4(x)=0,\quad \frac{\partial M_Y}{\partial x}-Q_Z+\bar{M}_5(x)=0, \tag{1d–e}$$

$$-\frac{\partial}{\partial x}[T_{\mathrm{SV}}+T_W]+\bar{M}_6(x)=0,\quad \frac{\partial B}{\partial x}-T_W+\bar{M}_7(x)=0, \tag{1f–g}$$

where Q_X is the axial force; Q_Y and Q_Z are shear forces; M_Y and M_Z are bending moments, B is the bimoment, T_{SV} is the twisting moment due to pure torsion and T_W is the flexural–torsional moment, due to warping torsion. $\bar{M}_j, j=1,\ldots,7$ are the inertial forces. Eq. (1) define the extensional motion; Eqs. (1b) and (1c) define the bending motion in the plane XY; Eqs. (1d) and (1e) define the bending motion in the plane XZ; Eqs. (1f) and (1g) define the warping and twisting motion.

These differential equations may be subjected to the following boundary conditions:

(a) Clamped–clamped:

$$u_{xc}=u_{yc}=u_{zc}=\theta_z=\theta_y=\phi_x=\theta_x=0 \quad \text{at } x=0 \text{ and } x=L. \tag{2a,b}$$

(b) Clamped–free:

$$\begin{aligned} &u_{xc}=u_{yc}=u_{zc}=\theta_z=\theta_y=\phi_x=\theta_x=0 \quad \text{at } x=0,\\ &Q_X=Q_Y=Q_Z=M_Y=M_Z=T_{SV}+T_W=B=0 \quad \text{at } x=L. \end{aligned} \tag{3a,b}$$

(c) Simply supported for bending, free to warp and free to extend at one end:

$$\begin{aligned} &u_{xc}=u_{yc}=u_{zc}=\phi_x=M_Y=M_Z=B=0 \quad \text{at } x=0,\\ &u_{yc}=u_{zc}=\phi_x=Q_X=M_Y=M_Z=B=0 \quad \text{at } x=L. \end{aligned} \tag{4a,b}$$

In the previous equations, u_{xc} is the axial displacement of the centroid, u_{yc} and u_{zc} are lateral displacements of the centroid, θ_y and θ_z are the bending rotation parameters, ϕ_x is the twisting angle and θ_x is the warping intensity variable. In Appendix B, one can find a brief deduction of the differential equations (1) starting from the displacement field defined in Refs. [14,17].

For a general lamination, the aforementioned beam-stress-resultants are related to the displacement variables by means of the following expression [14,17]:

$$\begin{Bmatrix} Q_X\\ M_Y\\ M_Z\\ B\\ Q_Y\\ Q_Z\\ T_W\\ T_{SV} \end{Bmatrix} = \begin{bmatrix} J_{11}^{11} & J_{12}^{11} & J_{13}^{11} & J_{14}^{11} & J_{15}^{16} & J_{16}^{16} & J_{17}^{16} & J_{18}^{16}\\ & J_{22}^{11} & J_{23}^{11} & J_{24}^{11} & J_{25}^{16} & J_{26}^{16} & J_{27}^{16} & J_{28}^{16}\\ & & J_{33}^{11} & J_{34}^{11} & J_{35}^{16} & J_{36}^{16} & J_{37}^{16} & J_{38}^{16}\\ & & & J_{44}^{11} & J_{45}^{16} & J_{46}^{16} & J_{47}^{16} & J_{48}^{16}\\ & & & & J_{55}^{66} & J_{56}^{66} & J_{57}^{66} & J_{58}^{66}\\ & & \text{sym} & & & J_{66}^{66} & J_{67}^{66} & J_{68}^{66}\\ & & & & & & J_{77}^{66} & J_{78}^{66}\\ & & & & & & & J_{88}^{66} \end{bmatrix} \begin{Bmatrix} u'_{xc}\\ -\theta'_y\\ -\theta'_z\\ -\theta'_x\\ u'_{yc}-\theta_z\\ u'_{zc}-\theta_y\\ \phi'_x-\theta_x\\ \phi'_x \end{Bmatrix} \tag{5}$$

and the inertia terms are expressed as follows:

$$\begin{Bmatrix} \bar{M}_1 \\ \bar{M}_2 \\ \bar{M}_3 \\ \bar{M}_4 \\ \bar{M}_5 \\ \bar{M}_6 \\ \bar{M}_7 \end{Bmatrix} = \begin{bmatrix} J_{11}^{\rho} & 0 & 0 & 0 & 0 & 0 & 0 \\ & J_{11}^{\rho} & 0 & 0 & 0 & 0 & 0 \\ & & J_{33}^{\rho} & 0 & 0 & 0 & 0 \\ & & & J_{11}^{\rho} & 0 & 0 & 0 \\ & & & & J_{22}^{\rho} & 0 & 0 \\ & \text{sym} & & & & J_{22}^{\rho}+J_{33}^{\rho} & 0 \\ & & & & & & J_{44}^{\rho} \end{bmatrix} \begin{Bmatrix} \ddot{u}_{xc} \\ \ddot{u}_{yc} \\ \ddot{\theta}_z \\ \ddot{u}_{zc} \\ \ddot{\theta}_y \\ \ddot{\phi}_x \\ \ddot{\theta}_x \end{Bmatrix}. \tag{6}$$

The stiffness coefficients in Eq. (5) and the inertia coefficients in Eq. (6) are obtained as follows:

$$J_{ij}^{kh} = \int_S \left[\bar{A}_{kh}\left(\bar{g}_i^{(a)}\bar{g}_j^{(a)}\right) + \bar{B}_{kh}\left(\bar{g}_i^{(a)}\bar{g}_j^{(c)} + \bar{g}_i^{(c)}\bar{g}_j^{(a)}\right) + \bar{D}_{kh}\left(\bar{g}_i^{(c)}\bar{g}_j^{(c)}\right)\right] \mathrm{d}s,$$

$$J_{ij}^{\rho} = \int_A \rho \bar{g}_i^{(d)}\bar{g}_j^{(d)}\,\mathrm{d}s\,\mathrm{d}n, \tag{7a,b}$$

where the vectors $\bar{g}^{(j)}$ are defined as follows:

$$\bar{g}^{(a)} = \left\{1, Z(s), Y(s), \omega_P, \frac{\mathrm{d}Y}{\mathrm{d}s}, \frac{\mathrm{d}Z}{\mathrm{d}s}, r(s)+\psi(s), \psi(s)\right\},$$

$$\bar{g}^{(c)} = \left\{0, \frac{\mathrm{d}Y}{\mathrm{d}s}, -\frac{\mathrm{d}Z}{\mathrm{d}s}, l(s), 0, 0, 1, -2\right\}, \quad \bar{g}^{(d)} = \left\{1, Z(s)+n\frac{\mathrm{d}Y}{\mathrm{d}s}, Y(s)-n\frac{\mathrm{d}Z}{\mathrm{d}s}, \omega(s)\right\}. \tag{8a - c}$$

In the Eq. (7), ρ is the density and $\bar{A}_{ij}$, $\bar{B}_{ij}$ and $\bar{D}_{ij}$ are modified elastics coefficients (see Appendix B, [10,14]), whereas ω is the whole warping function, which is composed by two terms: primary or contour warping (ω_p) and secondary or thickness warping (ω_s) defined by

$$\omega = \omega_p(s) + \omega_s(s,n), \quad \omega_p(s) = \int_{s_0}^{s} [r(s)+\psi(s)]\,\mathrm{d}s - D_C, \quad \omega_s(s,n) = nl(s). \tag{9}$$

The function $\psi(s)$ is the shear flow of pure torsion (or Saint Venant torsion) for a closed contour section. It accounts for variable laminates along the contour and it is defined as follows:

$$\psi(s) = \frac{1}{\bar{A}_{66}(s)}\left[\frac{\int_s r(s)\,\mathrm{d}s}{\oint_S (1/\bar{A}_{66}(s))\,\mathrm{d}s}\right], \quad D_C = \frac{\oint_S [r(s)+\psi(s)]\bar{A}_{11}(s)\,\mathrm{d}s}{\oint_S \bar{A}_{11}(s)\,\mathrm{d}s}. \tag{10a,b}$$

In the case of an open cross-section $\psi(s) = 0$. The functions $r(s)$ and $l(s)$ are defined as follows:

$$r(s) = Z(s)\frac{\mathrm{d}Y}{\mathrm{d}s} - Y(s)\frac{\mathrm{d}Z}{\mathrm{d}s}, \quad l(s) = Y(s)\frac{\mathrm{d}Y}{\mathrm{d}s} + Z(s)\frac{\mathrm{d}Z}{\mathrm{d}s}, \tag{11a,b}$$

The stacking sequences of hypothesis (*f*) provide selective elastic couplings such as torsion-extension or bending-torsion even for cases of cross-section with double symmetry. The configurations CUS and CAS were adopted specifically for closed cross-sections by Rehfield et al. [6]. There are many different stacking sequences that show evidence of the elastic couplings manifested by CUS and CAS configurations. In Fig. 3a and b one can see a class of CUS and CAS configurations, respectively. The fiber-reinforcement angle α is arranged according Fig. 2d.

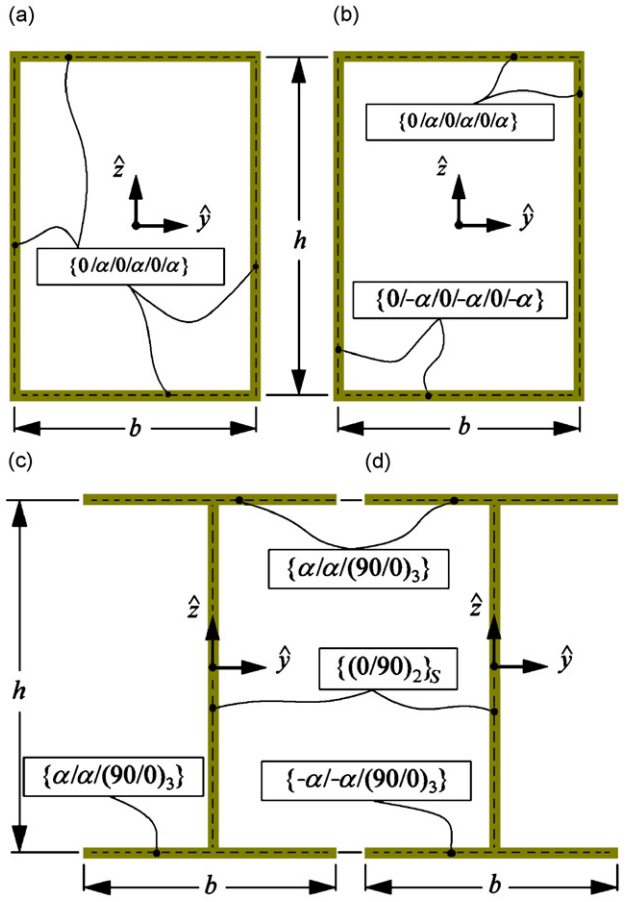

Fig. 3. (a) CUS and (b) CAS lamination for closed rectangular section. (c) CUS-like and (d) CAS-like lamination for open I-cross-section.

The CAS configuration has the following beam stress–strain relations [14]:

$$\begin{Bmatrix} Q_X \\ M_Y \\ M_Z \\ B \\ Q_Y \\ Q_Z \\ T_W \\ T_{SV} \end{Bmatrix} = \begin{bmatrix} J_{11}^{11} & 0 & 0 & 0 & J_{15}^{16} & J_{16}^{16} & 0 & 0 \\ 0 & J_{22}^{11} & 0 & 0 & 0 & 0 & J_{27}^{16} & J_{28}^{16} \\ 0 & 0 & J_{33}^{11} & 0 & 0 & 0 & J_{37}^{16} & J_{38}^{16} \\ 0 & 0 & 0 & J_{44}^{11} & 0 & 0 & 0 & 0 \\ J_{15}^{16} & 0 & 0 & 0 & J_{55}^{66} & 0 & 0 & 0 \\ J_{16}^{16} & 0 & 0 & 0 & 0 & J_{66}^{66} & 0 & 0 \\ 0 & J_{27}^{16} & J_{37}^{16} & 0 & 0 & 0 & J_{77}^{66} & J_{78}^{66} \\ 0 & J_{28}^{16} & J_{38}^{16} & 0 & 0 & 0 & J_{78}^{66} & J_{88}^{66} \end{bmatrix} \begin{Bmatrix} u'_{xc} \\ -\theta'_y \\ -\theta'_z \\ -\theta'_x \\ u'_{yc} - \theta_z \\ u'_{zc} - \theta_y \\ \phi'_x - \theta_x \\ \phi'_x \end{Bmatrix}. \tag{12}$$

This expression implies, according to the constitutive behavior, that torsion induces fully coupled bending and extension. In fact, the CAS configuration shown in Fig. 3b, produces elastic couplings between extension and shear forces because $J_{15}^{16} \neq 0$ and $J_{16}^{16} \neq 0$. The torsion motion is coupled with the bending moments due to the non-vanishing coefficients J_{27}^{16}, J_{28}^{16}, J_{37}^{16} and J_{38}^{16}. In a few words, the torsion moments (and ϕ_x and θ_x) are elastically coupled with the bending moments (and θ_y and θ_z) that by equilibrium are connected with the shear forces (and u_y and u_z) that are elastically coupled with the extensional force (and u_x).

The CUS configuration has the following beam stress–strain relations [14]:

$$\begin{Bmatrix} Q_X \\ M_Y \\ M_Z \\ B \\ Q_Y \\ Q_Z \\ T_W \\ T_{SV} \end{Bmatrix} = \begin{bmatrix} J_{11}^{11} & 0 & 0 & 0 & 0 & 0 & J_{17}^{16} & J_{18}^{16} \\ 0 & J_{22}^{11} & 0 & 0 & J_{25}^{16} & 0 & 0 & 0 \\ 0 & 0 & J_{33}^{11} & 0 & 0 & J_{36}^{16} & 0 & 0 \\ 0 & 0 & 0 & J_{44}^{11} & 0 & 0 & 0 & 0 \\ 0 & J_{25}^{16} & 0 & 0 & J_{55}^{66} & 0 & 0 & 0 \\ 0 & 0 & J_{36}^{16} & 0 & 0 & J_{66}^{66} & 0 & 0 \\ J_{17}^{16} & 0 & 0 & 0 & 0 & 0 & J_{77}^{66} & J_{78}^{66} \\ J_{18}^{16} & 0 & 0 & 0 & 0 & 0 & J_{78}^{66} & J_{88}^{66} \end{bmatrix} \begin{Bmatrix} u'_{xc} \\ -\theta'_y \\ -\theta'_z \\ -\theta'_x \\ u'_{yc} - \theta_z \\ u'_{zc} - \theta_y \\ \phi'_x - \theta_x \\ \phi'_x \end{Bmatrix}. \tag{13}$$

Eq. (13) indicates that extension induces torsion. In this case, the axial force Q_X is coupled with the torsional moments T_W and T_{SV} due to the non-vanishing coefficients J_{17}^{16} and J_{18}^{16}. On the other hand the bending moments M_Z and M_Y are coupled with the shear forces Q_Z and Q_Y, by means of the non-vanishing coefficients J_{25}^{16} and J_{36}^{16}, respectively. Thus, a bending action (force or moment) in the XY plane induces bending in the XZ plane and vice versa.

Although the names CUS and CAS are proper denominations for stacking sequences of closed cross-sections, the lamination sequence of the open cross-sections can be arranged in order to have the same or similar elastic couplings of the closed cross-section counterpart. Thus, the stacking sequences of Fig. 3c and d have a similar elastic behavior as the CUS and CAS configurations, respectively. In fact, according to the stacking sequence of Fig. 3c one has an elastic coupling quite similar to the CUS configuration because the torsion moments are coupled with the axial force Q_X by means of the non-vanishing coefficients J_{17}^{16} and J_{18}^{16}, and the bending moment M_Y is coupled with the shear force Q_Y by means of non-vanishing coefficient J_{25}^{16}. On the other hand, the stacking sequence of Fig. 3d manifests an elastic coupling quite similar to the CAS configuration because the torsion moments are coupled with the bending moment M_Y by means of the coefficients J_{27}^{16} and J_{28}^{16}, and the axial force Q_X is coupled with the shear force Q_Y by means of the coefficient J_{15}^{16}.

If $\alpha = 90^\circ$ or $\alpha = 0^\circ$, the CAS and CUS configurations of Fig. 3 coincide with a cross-ply configuration which decouples the bending, extensional and torsion movements because in this case the coefficients of constitutive matrix in Eq. (5) are such that $J_{ij}{}^{16} = 0$ and $J_{ij}{}^{66} = 0\ \forall i \neq j$, but $J_{78}^{66} \neq 0$ (this is inherent to the model as one can see in Refs. [10,14]). Then, under these circumstances, the eigenvalues for CAS, CUS and cross-ply configurations are the same.

3. Power series methodology

The exact solution of the present eigenvalue problem is carried out by means of a generalization of the power series scheme developed originally by Filipich et al. [18,19] and Rosales and Filipich [20] for structural problems involving isotropic materials. The methodology requires a previous non-dimensional re-definition of the differential equations, which implies that $\bar{x} \in [0, 1]$, with $\bar{x} = x/L$ [18].

The displacement variables have the common harmonic motion:

$$\{u_{xc}, u_{yc}, \theta_z, u_{zc}, \theta_y, \phi_x, \theta_x\} = \{u_1, u_2, u_3, u_4, u_5, u_6, u_7\}\, \mathrm{e}^{\mathrm{i}\Omega t} = \bar{u}\mathrm{e}^{\mathrm{i}\Omega t}, \tag{14}$$

where Ω is the circular frequency measured in rad/seg, t is the temporal variable and $\mathrm{i} = \sqrt{-1}$, whereas the generic displacement $u_i(\bar{x})$ is expanded with the following power series:

$$u_i = \sum_{k=0}^{M} \widehat{C}_{ik} \bar{x}^k, \quad i = 1, \ldots, 7, \tag{15}$$

where the $\widehat{C}_{ik}$'s are unknowns coefficients. Theoretically $M \to \infty$, however, for practical purposes M may be an arbitrary large integer.

Now, taking into account the harmonic motion of Eq. (14) and the non-dimensional re-definition of the domain and variables, the eigenvalue problem derived from Eq. (1) may be written in the following second-order differential system:

$$\sum_{j=1}^{7} f_{ij}(\bar{x})u_j''(\bar{x}) + \hat{F}_i(\bar{u},\bar{u}') + \lambda u_i(\bar{x}) = 0, \quad i = 1,\ldots,7 \quad \text{and} \quad \bar{x} \in [0,1]. \tag{16}$$

The functions $f_{ij}(\bar{x})$ and $\hat{F}_i(\bar{u},\bar{u}')$ which are considered analytic $\forall \bar{x} \in [0,1]$ condense the variation of the cross-section geometric properties (width and/or height) together with the Eq. (5). These functions can be defined in the following form:

$$f_{ij}(\bar{x}) = \sum_{k=0}^{M} a_{ijk}\bar{x}^k, \quad i,j = 1,\ldots,7, \tag{17}$$

$$\hat{F}_i(\bar{u},\bar{u}') = \sum_{j=1}^{7}[w_{ij}(\bar{x})u_i'(\bar{x}) + v_{ij}(\bar{x})u_i(\bar{x})], \quad i = 1,\ldots,7, \tag{18}$$

where $w_{ij}(\bar{x})$ and $v_{ij}(\bar{x})$ are functions depending on the cross-sectional dimensions and lamination type. The eigenvalue λ is related to the circular frequency by means of the following expression:

$$\lambda = \Omega\sqrt{\rho e L}. \tag{19}$$

The boundary conditions can be expressed in the following generic form:

$$\bar{\alpha}_{0i}u_i(0) + \bar{\beta}_{0i}u_i'(0) = 0, \quad i = 1,\ldots,7, \tag{20a}$$

$$\bar{\alpha}_{1i}u_i(1) + \bar{\beta}_{1i}u_i'(1) = 0, \quad i = 1,\ldots,7, \tag{20b}$$

where the coefficients $\bar{\alpha}_{ni}$ and $\bar{\beta}_{ni}$, $n = 0,1$, $i = 1,\ldots,7$ are given according to Eqs. (2)–(4).

Now, substituting Eq. (15) in Eq. (20) one has the equations of boundary conditions described in terms of the unknown coefficients $\widehat{C}_{ik}$'s, as shown in the following equation:

$$\bar{\alpha}_{0i}\widehat{C}_{i0} + \bar{\beta}_{0i}\widehat{C}_{i1} = 0, \quad i = 1,\ldots,7, \tag{21a}$$

$$\bar{\alpha}_{1i}\sum_{k=0}^{M}\widehat{C}_{ik} + \bar{\beta}_{1i}\sum_{k=0}^{M-1}(k+1)\widehat{C}_{i(k+1)} = 0, \quad i = 1,\ldots,7. \tag{21b}$$

In view of the fact that in the present problem the cross-section properties vary continuously along the domain leading to a second-order differential system with variable coefficients, therefore one has to employ power series products together with the power series form of higher derivatives. Then it is important to keep in mind the following two remarks:

Remark 1. If $h_1(\bar{x}), h_2(\bar{x})$ and $h_3(\bar{x})$ are analytic functions defined by the following power series:

$$h_n(\bar{x}) = \sum_{k=0}^{M} C_{nk}\bar{x}^k, \quad n = 1,2,3, \tag{22}$$

and if $h_n(\bar{x})$, $n = 1,2,3$ are such that $h_3(\bar{x}) = h_1(\bar{x})h_2(\bar{x})$ and remembering the concept of Cauchy products, then one can easily see that:

$$C_{3k} = \sum_{m=0}^{k} C_{1m}C_{2(k-m)} = \sum_{m=0}^{k} C_{2m}C_{1(k-m)}. \tag{23}$$

Remark 2. If $h_1(\bar{x})$ is defined according to Eq. (22), then the mth-order derivative is given by

$$\frac{\mathrm{d}^m h_1(\bar{x})}{\mathrm{d}\bar{x}^m} = \sum_{k=0}^{M-m}\varphi_{mk}C_{1(m+k)}\bar{x}^k, \quad \text{where} \quad \varphi_{mk} = (k+1)(k+2)\ldots(k+m) = \frac{(k+m)!}{k!}, \tag{24}$$

Now, substituting Eq. (15) into Eq. (16) one can simplify the terms as follows:

$$\sum_{j=1}^{7} f_{ij}(\bar{x})u_j''(\bar{x}) = \sum_{k=0}^{M-2} P_{ik}\bar{x}^k, \quad i = 1,\ldots,7, \tag{25a}$$

$$\sum_{j=1}^{7} [w_{ij}(\bar{x})u_j'(\bar{x}) + v_{ij}(\bar{x})u_j(\bar{x})] = \sum_{k=0}^{M-1} F_{ik}\bar{x}^k, \quad i = 1,\ldots,7, \tag{25b}$$

where

$$P_{ik} = \sum_{r=0}^{k} \varphi_{2r} \sum_{j=1}^{7} \widehat{C}_{j(r+2)} a_{ij(k-r)}, \quad i = 1,\ldots,7, \quad k = 0,1,\ldots M-2 \tag{26}$$

and the differential system can be expressed, in terms of the unknown coefficients $\widehat{C}_{ik}$'s, in the following form (for F_{ik} see Remark 1):

$$P_{ik} + F_{ik} + \lambda \widehat{C}_{ik} = 0, \quad i = 1,\ldots,7, \quad k = 0,1,\ldots M-2. \tag{27}$$

Now, to obtain a recurrence scheme for the $\widehat{C}_{ik}$'s, note that Eq. (26) may be expressed as

$$P_{ik} = P_{ik}^* + \varphi_{2k} \sum_{j=1}^{7} \widehat{C}_{j(k+2)} a_{ij0}, \quad i = 1,\ldots,7, \quad k = 0,1,\ldots,M-2 \tag{28}$$

with

$$P_{ik}^* = \sum_{r=0}^{k-1} \varphi_{2r} \sum_{j=1}^{7} \widehat{C}_{j(r+2)} a_{ij(k-r)}, \quad i = 1,\ldots,7, \quad k = 0,1,\ldots,M-2. \tag{29}$$

Note that Eq. (29) is simply the Eq. (26) where the upper limit of the summation in r is reduced in one. Then, the system defined in Eq. (27) can be rearranged in terms of the $\widehat{C}_{j(r+2)}$'s as

$$\sum_{j=1}^{7} \widehat{C}_{j(k+2)} a_{ij0} = -\frac{1}{\varphi_{2k}} (P_{ik}^* + F_{ik} + \lambda \widehat{C}_{ik}), \quad i = 1,\ldots,7, \quad k = 0,1,\ldots M-2. \tag{30}$$

Now solving, for each "k", the 7×7 system defined in Eq. (30) in the unknowns $\widehat{C}_{j(k+2)}$, $j = 1,\ldots,7$ one obtains the aforementioned recurrence scheme. Note that the recurrence scheme implies that for each "k", the coefficients $\widehat{C}_{i(k+2)}$, $i = 1,\ldots,7$, depends on the other coefficients $\widehat{C}_{in}$, $i = 1,\ldots,7$, with $n < k+2$. At the beginning when $k = 0$, one needs to know the fourteen coefficients $\widehat{C}_{i0}$ and $\widehat{C}_{i1}$, $i = 1,\ldots,7$ involved in the boundary condition of Eq. (21a), and simultaneously one has to satisfy the Eq. (21b). Then one can proceed as follows:

(1) Seven of the fourteen coefficients $\widehat{C}_{i0}$ and $\widehat{C}_{i1}$, $i = 1,\ldots,7$, are conveniently selected (i.e. according to the form of the boundary equation). These seven coefficients denominated "free coefficients", are defined as γ_i, $i = 1,\ldots,7$.
(2) According to the linearity of the present problem one can appeal to the principle of superposition, performing alternatively the following seven forms:

$$\begin{aligned}
&\gamma_1 = 1, \quad \gamma_2 = \gamma_3 = \gamma_4 = \gamma_5 = \gamma_6 = \gamma_7 = 0,\\
&\gamma_2 = 1, \quad \gamma_1 = \gamma_3 = \gamma_4 = \gamma_5 = \gamma_6 = \gamma_7 = 0,\\
&\gamma_3 = 1, \quad \gamma_1 = \gamma_2 = \gamma_4 = \gamma_5 = \gamma_6 = \gamma_7 = 0,\\
&\gamma_4 = 1, \quad \gamma_1 = \gamma_2 = \gamma_3 = \gamma_5 = \gamma_6 = \gamma_7 = 0,\\
&\gamma_5 = 1, \quad \gamma_1 = \gamma_2 = \gamma_3 = \gamma_4 = \gamma_6 = \gamma_7 = 0,\\
&\gamma_6 = 1, \quad \gamma_1 = \gamma_2 = \gamma_3 = \gamma_4 = \gamma_5 = \gamma_7 = 0,\\
&\gamma_7 = 1, \quad \gamma_1 = \gamma_2 = \gamma_3 = \gamma_4 = \gamma_5 = \gamma_6 = 0.
\end{aligned} \tag{31}$$

(3) For each of the seven alternatives described in Eq. (31), one can apply the recurrence form defined in Eq. (30) for a given value of λ to obtain $\widehat{C}_{i2}, \widehat{C}_{i3}, \ldots, \widehat{C}_{in}$, $i = 1,\ldots,7$, which afterwards are substituted in the seven boundary conditions of Eq. (21b). The resulting expressions of these boundary conditions leads to the following homogeneous system in the unknowns γ_i, $i = 1,\ldots,7$:

$$\begin{bmatrix} \varepsilon_{11}(\lambda) & \varepsilon_{12}(\lambda) & \varepsilon_{13}(\lambda) & \varepsilon_{14}(\lambda) & \varepsilon_{15}(\lambda) & \varepsilon_{16}(\lambda) & \varepsilon_{17}(\lambda) \\ \varepsilon_{21}(\lambda) & \varepsilon_{22}(\lambda) & \varepsilon_{23}(\lambda) & \varepsilon_{24}(\lambda) & \varepsilon_{25}(\lambda) & \varepsilon_{26}(\lambda) & \varepsilon_{27}(\lambda) \\ \varepsilon_{31}(\lambda) & \varepsilon_{32}(\lambda) & \varepsilon_{33}(\lambda) & \varepsilon_{34}(\lambda) & \varepsilon_{35}(\lambda) & \varepsilon_{36}(\lambda) & \varepsilon_{37}(\lambda) \\ \varepsilon_{41}(\lambda) & \varepsilon_{42}(\lambda) & \varepsilon_{43}(\lambda) & \varepsilon_{44}(\lambda) & \varepsilon_{45}(\lambda) & \varepsilon_{46}(\lambda) & \varepsilon_{47}(\lambda) \\ \varepsilon_{51}(\lambda) & \varepsilon_{52}(\lambda) & \varepsilon_{53}(\lambda) & \varepsilon_{54}(\lambda) & \varepsilon_{55}(\lambda) & \varepsilon_{56}(\lambda) & \varepsilon_{57}(\lambda) \\ \varepsilon_{61}(\lambda) & \varepsilon_{62}(\lambda) & \varepsilon_{63}(\lambda) & \varepsilon_{64}(\lambda) & \varepsilon_{65}(\lambda) & \varepsilon_{66}(\lambda) & \varepsilon_{67}(\lambda) \\ \varepsilon_{71}(\lambda) & \varepsilon_{72}(\lambda) & \varepsilon_{73}(\lambda) & \varepsilon_{74}(\lambda) & \varepsilon_{75}(\lambda) & \varepsilon_{76}(\lambda) & \varepsilon_{77}(\lambda) \end{bmatrix} \begin{Bmatrix} \gamma_1 \\ \gamma_2 \\ \gamma_3 \\ \gamma_4 \\ \gamma_5 \\ \gamma_6 \\ \gamma_7 \end{Bmatrix} = \begin{Bmatrix} 0 \\ 0 \\ 0 \\ 0 \\ 0 \\ 0 \\ 0 \end{Bmatrix}, \tag{32}$$

where $\varepsilon_{ij}(\lambda)$ represent the ith boundary condition defined according to Eq. (21b) that corresponds to the jth alternative of Eq. (31).

(4) Finally, if λ is the appropriate eigenvalue, then the following characteristic equation is satisfied:

$$\det[\varepsilon_{ij}(\lambda)] = 0. \tag{33}$$

The recurrence scheme, as shown in the previous paragraphs, allows to shrink the algebraic problem from $7(M+1)$ to only 7 unknown coefficients that can be selected according to the boundary equations.

It has to be pointed out that the present power series scheme can be strongly simplified in some cases of stacking sequences. This fact leads to the handling of two, three or four subsystems. For example in the case of special orthotropic configurations one can handle three subsystems of two equations (twisting motion, flapwise motion and chordwise motion) and the remaining equation (for extension). In the case of a CUS configuration one can handle two subsystems, i.e. a subsystem with three equations (extension and twisting due to pure torsion and warping torsion) and a subsystem with four equations (flapwise bending, chordwise bending, flapwise shear and chordwise shear). General configurations and even the CAS configuration lead to a full coupling (extensional, twisting, flapwise-chordwise bending and shear), and therefore to the handling of the full system of seven equations. On the other hand due to the linearity of the present model the principle of superposition has been employed in the power series methodology.

4. Numerical studies and analysis

In this section numerical studies on beams that have a variable web height h and constant flanges b and thickness e are performed. The height for both open and closed cross-sections is assumed to have the linear variation given in the following expression:

$$h(\bar{x}) = h_o - \beta\bar{x}. \tag{34}$$

The beam has a unit length and many height/length, width/height and thickness/height ratios are employed. In the calculation scheme, power series of 50 terms ($M = 50$) are employed. In Table 1 the properties of the graphite fiber reinforced epoxy AS4/3501-6 are summarized.

4.1. Comparisons of models and tests of earlier finite element procedures

Table 2 shows the first five frequencies of a tapered composite box-beam with a particular CUS stacking sequence of $\{0/-45/45/90\}_S$ calculated with 400 SHELL4T elements of COSMOS/M and with the present power series solution ($M = 50$) of the beam model. The geometric properties are such that $h_o/L = 0.1$, $b/h_o = 0.6$, $e/h_o = 0.06$ and $\beta = 0.04$. One can see a good agreement between the solution of the beam model and the shell approach, even in the case of an important taper ratio.

The eigenvalues with the power series methodology are a straightforward test for the quality of finite elements. Thus, in Table 3 a study of the convergence quality of a finite element previously developed [17] for the present beam model is carried out. The geometric properties are such that $h_o/L = 0.1$, $b/h_o = 0.6$, $e/h_o = 0.03$, $\beta = 0.04$ and $\alpha = 15^\circ$ in the CAS lamination of Fig. 3b. One can see that the eigenvalues calculated with the finite element approach converge monotonically to the exact solution furnished with the power series methodology. Moreover, although the finite element approach is good enough for practical purposes, even with 200 elements the approximation doesn't reach the exact values given by the power series methodology. Now, in the following paragraphs new parametric studies of the effect of taper, lamination sequences and slenderness in the coupled vibrations of thin-walled composite beams are offered.

4.2. Analysis of elastic couplings in closed cross-section

In Table 4 the circular frequencies for clamped–free beams with closed cross-section ($b/h_o = 0.6$, $e/h_o = 0.06$, $\beta = 0.04$ and $\alpha = 15^\circ$) with CUS and CAS configuration and for different slenderness ratios h_o/L are summarized. It is interesting to note that the eigenvalues of CAS and CUS configurations manifest differences of no more than 10% between them. However the mode shapes of the corresponding frequencies of

Table 1
Mechanic properties of the materials employed in the paper

$E_1 = 144\,\text{GPa}$, $E_2 = 9.68\,\text{GPa}$
$G_{12} = G_{13} = 4.14\,\text{GPa}$, $G_{23} = 3.45\,\text{GPa}$
$\nu_{12} = 0.3$, $\nu_{23} = 0.5$
$\rho = 1389\,\text{kg/m}^3$

Table 2
Comparison of a two-dimensional shell model and the one-dimensional beam model, for a tapered composite box-beam

Boundaries	Method	Ω_1	Ω_2	Ω_3	Ω_4	Ω_5
Clamped–clamped	Shell: COSMOS/M	3234.3	3954.9	8049.9	9814.6	10004.5
	Beam: Power series	3237.0	3925.0	8114.3	9721.2	10262.1
Clamped–Free	Shell: COSMOS/M	614.3	842.9	3353.8	4266.7	5945.4
	Beam: Power series	613.0	836.8	3362.8	4232.8	5999.8

Natural frequencies Ω_k in rad/s.

Table 3
Convergence analysis of a former finite element [17]

Number of elements [14]	Ω_1	Ω_2	Ω_3	Ω_4	Ω_5
5	3538.8	4182.6	6416.4	7906.6	9266.4
10	3500.1	4128.9	6332.9	7628.9	8930.3
20	3483.0	4108.4	6311.6	7545.4	8835.9
30	3478.1	4103.4	6307.3	7524.7	8815.0
40	3475.9	4101.5	6305.5	7516.1	8806.8
60	3473.8	4100.0	6303.9	7509.1	8800.4
80	3472.8	4099.4	6303.1	7506.5	8798.1
100	3472.2	4099.1	6302.6	7505.2	8796.9
200	3471.1	4098.7	6301.5	7503.3	8795.3
Series	3469.8	4097.6	6301.3	7502.5	8794.5

Natural frequencies Ω_k in rad/s.

CAS and CUS configurations are quite different due to the elastic coupling allowed. Thus, Figs. 4 and 5 depict, for CAS and CUS configurations respectively, the variation of the frequencies (associated to a given mode shape) with respect to the slenderness ratio h_o/L. The frequencies and their associated modes shapes correspond to the example given in Table 4. The acronyms employed in Figs. 4 and 5 can be understood in the following way: the number indicates the frequency order (first, second, etc.); the first capital letter indicates the main contribution to the motion (T, F, E mean twisting motion, flexural motion, extensional motion); the letters after the hyphen indicate the motion direction and/or the kind of coupling: capitalized letters imply the direction of the main coupling. If capitalized letters appear alone, the mode shape is not coupled. That is, Y (or Z) alone implies the direction (normally for decoupled flexural modes), but xYz means coupled motion dominant in the y-direction). Thus, for the case $h_o/L = 0.1$ ($b/h_o = 0.6$, $e/h_o = 0.06$, $\beta = 0.04$ and $\alpha = 15°$), Fig. 6a shows the second fully coupled torsional/flexural/extensional mode (2°T-xYz) which has a coupled motion dominated by twisting and bending in the y-direction. The mode 2°T-xYz is typical of the CAS configuration. Fig. 6b shows the second coupled flexural mode (2°F-yZ) which has a motion pattern dominated by bending in the z-direction. The mode 2°F-yZ appears in CUS configurations. Fig. 6c shows the fully coupled first torsional/flexural/extensional mode (1°T-xyz) of the CAS configuration. The mode 1°T-xyz

Table 4
Natural frequencies of beams with closed sections having circumferentially asymmetric stiffness (CAS) and circumferentially uniform stiffness (CUS) laminations

Natural frequency (rad/s)	Type of lamination	h_o/L				
		0.050	0.075	0.100	0.125	0.150
Ω_1	CAS	488.0	663.7	836.3	996.8	1142.0
	CUS	479.2	653.1	821.1	976.1	1116.0
Ω_2	CAS	611.1	886.5	1136.6	1358.6	1551.1
	CUS	598.4	875.3	1123.6	1342.7	1532.8
Ω_3	CAS	2409.3	3229.2	3605.0	3549.2	3469.5
	CUS	2354.8	3237.5	3377.6	3248.7	3168.2
Ω_4	CAS	2516.3	3793.9	3981.2	4313.6	4604.8
	CUS	2493.4	3612.7	3867.0	4322.9	4658.3
Ω_5	CAS	4724.5	4172.9	4776.6	5360.8	5788.1
	CUS	4179.0	3852.5	4768.3	5391.0	5831.2

Natural frequencies Ω_k in rad/s. h_o/L is the slenderness ratio.

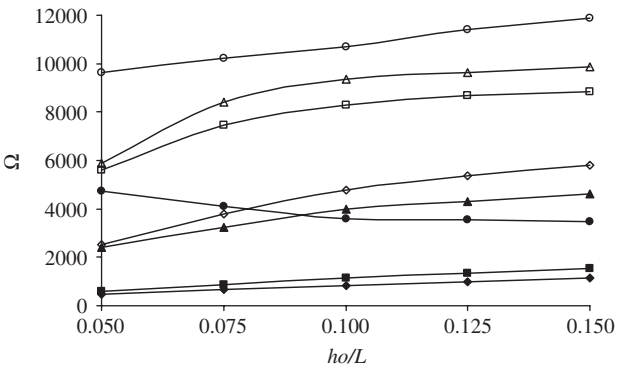

Fig. 4. Variation of frequencies associated to mode shapes with respect to the h_o/L ratio for a beam with closed cross-section with CAS configuration: (—◆—) 1°F-xYz; (—■—) 1°F-xyZ; (—▲—) 2°F-xYz; (—●—) 1°T-xyz; (—◇—) 2°F-xyZ; (—□—) 2°T-xYZ; (—△—) 2°T-xYz; (—○—) 3°T-xYz.

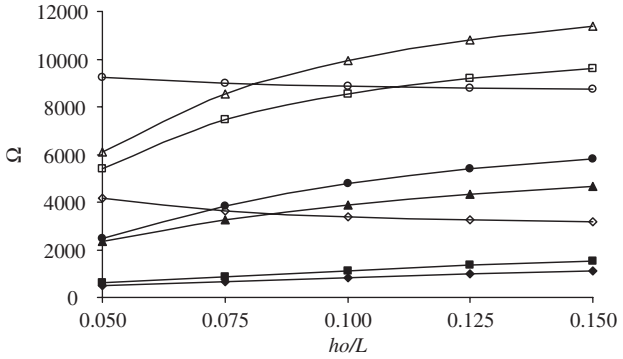

Fig. 5. Variation of frequencies associated to mode shapes with respect to the h_o/L ratio for a beam with closed cross-section with CUS configuration: (—◆—) 1°F-*Yz*; (—■—) 1°F-*yZ*; (—▲—) 2°F-*Yz*; (—●—) 2°F-*yZ*; (—◇—) 1°T-*E*; (—□—) 3°F-*Yz*; (—△—) 3°F-*yZ*; (—○—) 2°T-*E*.

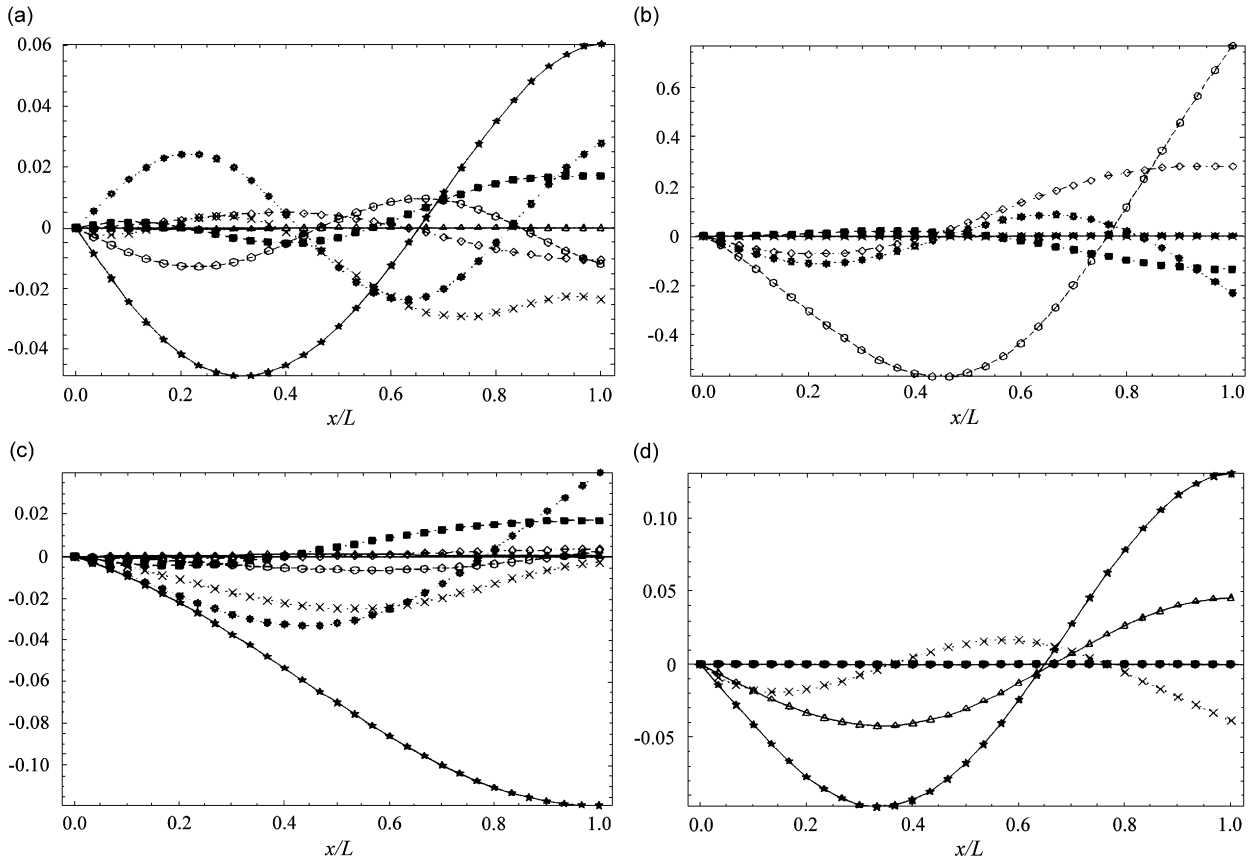

Fig. 6. (a) 2°T-*xYz* mode of the CAS configuration. (b) 2°F-*yZ* mode of the CUS configuration. (c) 1°T-*xyz* mode of the CAS configuration. (d) 1°T-*E* mode of the CUS configuration. All cases correspond to $h_o/L = 0.1$, $b/h_o = 0.6$, $e/h_o = 0.06$, $\beta = 0.04$ and $\alpha = 15°$. ( ) u_{xc}; (✲) u_{yc}; (■) θ_z; (⬡) u_{zc}; (◇)θ_y; (☆) ϕ_x; (╳) θ_x.

has a coupled motion dominated by twisting. Finally Fig. 6d shows the first torsional/extensional (1°T-*E*) mode of the CUS configuration (where the extensional displacement u_{xc} is plotted with a 100 × magnification in order to reveal the intensity of twisting/extension coupling). Moreover, in Figs. 4 and 5 one can see the phenomenon of mode crossover, which means that for a given order number of frequency its associated mode

shape experiments a qualitative change with the variation of a geometric parameter such as the slenderness ratio h_o/L.

Figs. 7 and 8 depict the variation of frequencies (associated to a specified mode) with respect to the taper ratio parameter β for clamped–free and clamped–clamped ends, respectively. The box-beam is such that $h_o/L = 0.05$, $b/h_o = 0.6$, $e/h_o = 0.06$, and $\alpha = 0^\circ$. Note that in the case with clamped–free ends; the twisting mode 1°T has two mode-crossovers with the bending modes 2°F-Y and 2°F-Z along the variation of the taper. In the case of the clamped–clamped ends the bending modes 1°F-Y and 1°F-Z and the bending modes 2°F-Y and 2°F-Z have mode-crossovers at $\beta = 0.035$. In Fig. 9 one can see the variation of frequencies with respect to the taper ratio for a clamped–clamped box-beam with the following features: $b/h_o = 0.6$, $e/h_o = 0.06$, CAS lamination with $\alpha = 30^\circ$, for $h_o/L = 0.05$ and $h_o/L = 0.15$. Now in Fig. 10 the variation of frequencies related to a given mode shape for a clamped–free box-beam is plotted. The geometric and lamination properties of this last case are: $b/h_o = 0.6$, $e/h_o = 0.06$, $\alpha = 0^\circ$.

After an examination of the evidence revealed in Figs. 4, 5, and 7–10 one can say that the presence of mode crossovers overlapping among the first frequencies of composite thin-walled tapered box-beams is connected with lower slenderness ratios, higher taper ratios and less restrictive boundary conditions.

4.3. Analysis of thin-walled beams with open cross-section

In Fig. 11 the variation of frequencies with respect to the taper ratio β of a clamped–free I-beam with a CUS-like stacking sequence is plotted. The beam is such that $h_o/L = 0.05$, $b/h_o = 0.6$, $e/h_o = 0.06$. Three

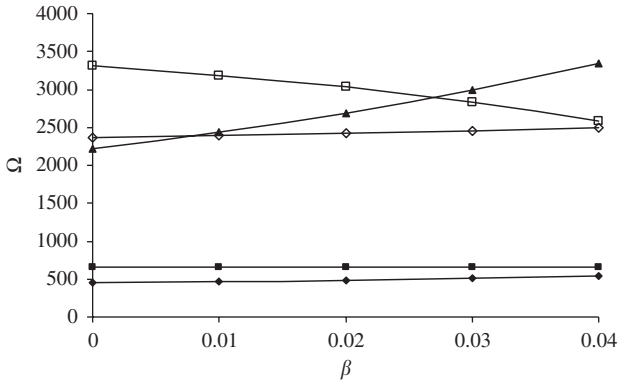

Fig. 7. Variation of frequencies with the taper ratio parameter β of a box-beam with $\alpha = 0$ and clamped–free boundary conditions: (—◆—) 1°F-Y; (—■—) 1°F-Z; (—▲—) 1°T; (—◇—) 2°F-Y; (—□—) 2°F-Z.

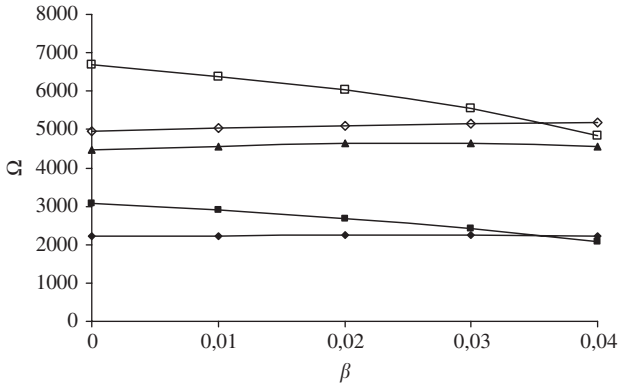

Fig. 8. Variation of frequencies with the taper ratio parameter β of a box-beam with $\alpha = 0$ and clamped–clamped boundary conditions: (—◆—) 1°F-Y; (—■—) 1°F-Z; (—▲—) 1°T; (—◇—) 2°F-Y; (—□—) 2°F-Z.

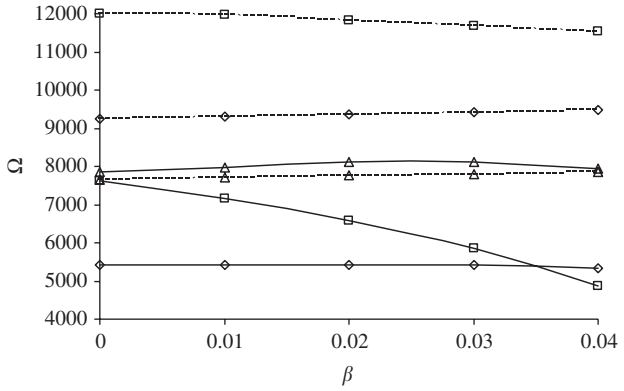

Fig. 9. Variation of frequencies with the taper ratio parameter β of a clamped–clamped box-beam with different slenderness ratios for CAS lamination $\alpha = 30^\circ$: continuous lines $h/L = 0.05$; dotted lines $h/L = 0.15$; (△) 1°T; (◇) 2°F-Y; (□) 2°F-Z.

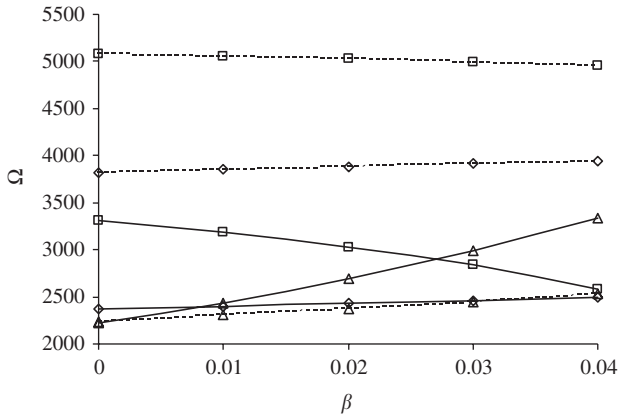

Fig. 10. Variation of frequencies with the taper ratio parameter β of a clamped–free box-beam with different slenderness ratios for $\alpha = 0^\circ$: continuous lines $h/L = 0.05$; dotted lines $h/L = 0.15$; (△) 1°T; (◇) 2°F-Y; (□) 2°F-Z.

different orientation angles are employed. Note the strong influence of the taper ratio in the twisting modes for each one of the stacking sequences studied. The frequencies related to the first twisting mode (1°T) for tapered beams can reach an increase of about 90% with respect to the uniform beam. On the other hand the frequencies related to the first flexural mode in the y-direction (1°F-Y) reach increments of about 18% and the frequencies associated to the first flexural mode in z-direction (1°F-Z) decrease in 6%. One can see the presence of a mode-crossover between 1°T and 1°F-Z modes in each stacking sequence.

In Fig. 12 the variation of frequencies with respect to the taper ratio β of a simply supported beam with a CAS-like configuration is shown. The geometric properties and the lamination features of this example are taken from the previous one. As it is possible to see, the frequencies associated to the first flexural mode in the y-direction (1°F-Y) reach increments of about 10% with respect to the uniform beam and the frequencies associated to the first flexural mode in the z-direction (1°F-Z) decrease about 40%, whereas frequencies related to the first twisting mode (1°T) can reach an increase of about 25% with respect to the case of uniform beam. In this case the mode-crossover between 1°T and 1°F-Z modes appear at higher values of the taper ratio β.

5. Conclusions

In this article quantitative and qualitative studies of the free vibrations of thin-walled tapered box-beams constructed with composite materials have been performed. Laminates providing special elastic couplings, like CUS and CAS stacking sequences have been employed. The effect of taper in the free vibrations of composite

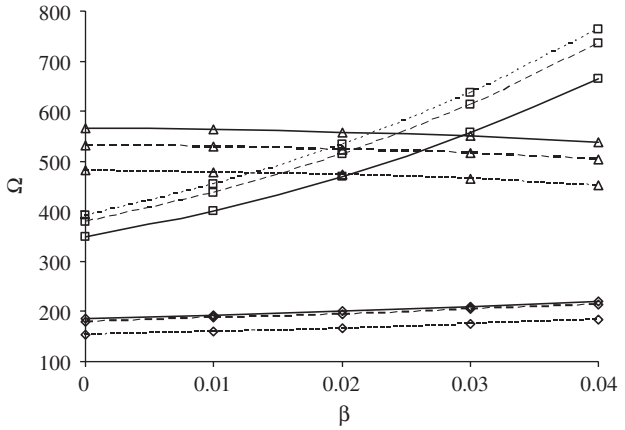

Fig. 11. Variation of frequencies with the taper ratio parameter β of a clamped–free I-beam with a CUS-like configuration for a slenderness ratio of $h_o/L = 0.05$: continuous lines $\alpha = 0°$; dashed lines $\alpha = 15°$; dotted lines $\alpha = 45°$; (△) 1°F-Z; (◇) 1°F-Y; (□) 1°T.

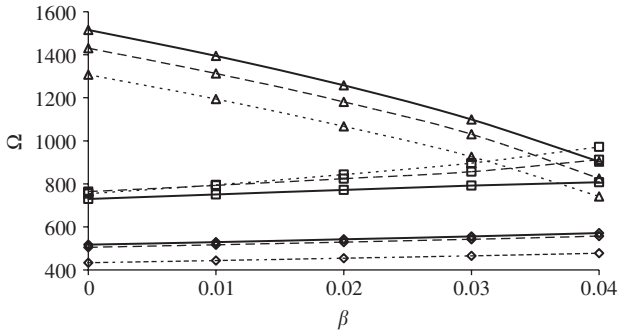

Fig. 12. Variation of frequencies with the taper ratio parameter β of a simply supported I-beam with a CAS-like configuration for a slenderness ratio of $h_o/L = 0.05$: continuous lines $\alpha = 0°$; dashed lines $\alpha = 15°$; dotted lines $\alpha = 45°$; (△) 1°F-Z; (◇) 1°F-Y; (□) 1°T.

thin-walled beams has been analyzed. The calculation process has been carried out appealing to a power series methodology, which gives exact (or with arbitrary precision) eigenvalues. In the calculation of the eigenvalues of composite tapered beams with linear or other functional variation along the domain, the power series methodology can offer advantages with respect to conventional finite element schemes where very fine meshes have to be used to get accurate results, especially to extract the higher modes. New parametric studies on the subject have been performed. These studies allow the qualitative analysis of composite tapered beams having the same dimensions but different elastic couplings. The tapering together with the coupling effects increase the presence of mode-crossovers between torsion dominant and bending dominant modes, in higher modes and even in lower modes. This fact is especially evident in the case of slender beams (i.e. for lower ratios of h_o/L), higher taper ratios and less restrictive boundary conditions.

Acknowledgments

The support of Secretaría de Ciencia y Tecnología de la Universidad Tecnológica Nacional and CONICET is greatly recognized.

Appendix A. Brief deduction of motion equations

The differential equations of this problem can be obtained be means of the principle of virtual work with an appropriate displacement field. The displacement field, compatible with the hypotheses summarized in the

second paragraph, is given in the following expression [14,17]:

$$\begin{aligned} u_x(x,y,z,t) &= u_{xc}(x,t) - \theta_z(x,t)y - \theta_y(x,t)z - \theta_x(x,t)\omega(s,n),\\ u_y(x,y,z,t) &= u_{yc}(x,t) - \phi_x(x,t)z,\\ u_z(x,y,z,t) &= u_{zc}(x,t) + \phi_x(x,t)y. \end{aligned} \tag{A.1}$$

The expression of the Principle of Virtual Work, compatible with the present problem, is

$$\iiint_V [\sigma_{xx}\delta\varepsilon^L_{xx} + \sigma_{xy}\delta\gamma^L_{xy} + \sigma_{xz}\delta\gamma^L_{xz}]\,\mathrm{d}V + \iiint_V \rho[\ddot{u}_x\delta u_x + \ddot{u}_y\delta u_y + \ddot{u}_z\delta u_z]\,\mathrm{d}V = 0, \tag{A.2}$$

where σ_{xx}, σ_{xy} and σ_{xz} are the stress components considered, ρ is the mass density, ε^L_{xx}, γ^L_{xy} and γ^L_{xz} are the components of the linear strain tensor that are given in terms of the displacement field variables by means of the following expression [14]:

$$\begin{aligned} \varepsilon^L_{xx} &= u'_{xc} - \theta'_z y - \theta'_y z - \theta'_x\omega,\\ \gamma^L_{xy} &= (u'_{yc} - \theta_z) - (z + \partial\omega/\partial y)\phi'_x + \partial\omega/\partial y(\phi'_x - \theta_x),\\ \gamma^L_{xz} &= (u'_{zc} - \theta_y) + (y - \partial\omega/\partial z)\phi'_x + \partial\omega/\partial z(\phi'_x - \theta_x). \end{aligned} \tag{A.3}$$

Remember that in Eqs. (A.2) and (A.3) the dots and apostrophes mean derivation with respect to the temporal variable 't' and spatial variable 'x', respectively. It is useful to define the beam stress resultants (or generalized forces and moment) in the following form:

$$\begin{aligned} \{Q_X, M_y, M_z, B\} &= \iint_A \sigma_{xx}\{1, z, y, \omega\}\,\mathrm{d}A,\\ \{Q_y, Q_z\} &= \iint_A \{\sigma_{xy}, \sigma_{xz}\}\,\mathrm{d}A,\\ \{T_{\mathrm{SV}}, T_W\} &= \iint_A \{\sigma_{xz}(y - \partial\omega/\partial z) - \sigma_{xy}(z + \partial\omega/\partial y), \sigma_{xy}\partial\omega/\partial y + \sigma_{xz}\partial\omega/\partial z\}\,\mathrm{d}A. \end{aligned} \tag{A.4}$$

Then, substituting (A.1), (A.3) and (A.4) in (A.2), collecting the like terms one has the following expression:

$$\begin{aligned} &\int_L [Q_X\delta u'_{xc} + Q_y\delta(u'_{yc} - \theta_z) + Q_z\delta(u'_{zx} - \theta_y) + T_W\delta(\phi'_x - \theta_x)]\,\mathrm{d}x + \int_L [T_W\delta\phi'_x - B\delta\theta'_x - M_y\delta\theta'_y - M_z\delta\theta'_z]\,\mathrm{d}x\\ &\quad + \int_L [\bar{M}_1\delta u_{xc} + \bar{M}_2\delta u_{yc} + \bar{M}_3\delta\theta_z + \bar{M}_4\delta u_{zc} + \bar{M}_5\delta\theta_y + \bar{M}_6\delta\phi_x + \bar{M}_7\delta\theta_x]\,\mathrm{d}x = 0. \end{aligned} \tag{A.5}$$

Finally, after performing in (A.5) the conventional steps of the variational calculus [14–17] one has the set of differential equations given in Eq. (1).

Appendix B. Reduced elastic coefficients

The stress–strain relations for a composite ply can be expressed in the following form [1,2]:

$$\begin{Bmatrix} \sigma_{xx}\\ \sigma_{ss}\\ \sigma_{nn}\\ \sigma_{sn}\\ \sigma_{xn}\\ \sigma_{xs} \end{Bmatrix} = \begin{bmatrix} \bar{Q}_{11} & \bar{Q}_{12} & \bar{Q}_{13} & 0 & 0 & \bar{Q}_{16}\\ \bar{Q}_{12} & \bar{Q}_{22} & \bar{Q}_{23} & 0 & 0 & \bar{Q}_{26}\\ \bar{Q}_{13} & \bar{Q}_{23} & \bar{Q}_{33} & 0 & 0 & \bar{Q}_{36}\\ 0 & 0 & 0 & \bar{Q}_{44} & \bar{Q}_{45} & 0\\ 0 & 0 & 0 & \bar{Q}_{45} & \bar{Q}_{55} & 0\\ \bar{Q}_{16} & \bar{Q}_{26} & \bar{Q}_{36} & 0 & 0 & \bar{Q}_{66} \end{bmatrix} \begin{Bmatrix} \varepsilon_{xx}\\ \varepsilon_{ss}\\ \varepsilon_{nn}\\ \gamma_{sn}\\ \gamma_{xn}\\ \gamma_{xs} \end{Bmatrix}. \tag{B.1}$$

In the above equation $\bar{Q}_{ij}$ are components of the transformed stiffness matrix defined [1,2] in terms of the elastic properties (elasticity moduli and Poisson coefficients) and fiber orientation of the ply [1,2]. Employing (B.1) and with the definition of shell stress resultants (B.2) and neglecting normal effects in thickness (i.e. $\sigma_{nn} = \varepsilon_{nn} = 0$) it is possible to obtain a constitutive form (B.3) in terms of shell stress resultants and shell

strain components [1]

$$\{N_{xx}, N_{ss}, N_{xs}, N_{xn}, N_{sn}, M_{xx}, M_{ss}, M_{xs}\} = \int_{-e/2}^{e/2} \{\sigma_{xx}, \sigma_{ss}, \sigma_{xs}, \sigma_{xn}, \sigma_{sn}, \sigma_{xx}n, \sigma_{ss}n, \sigma_{xs}n\}\, \mathrm{d}n \tag{B.2}$$

$$\begin{Bmatrix} N_{xx} \\ N_{ss} \\ N_{xs} \\ N_{sn} \\ N_{xn} \\ M_{xx} \\ M_{ss} \\ M_{xs} \end{Bmatrix} = \begin{bmatrix} A_{11} & A_{12} & A_{16} & 0 & 0 & B_{11} & B_{12} & B_{16} \\ A_{12} & A_{22} & A_{26} & 0 & 0 & B_{12} & B_{22} & B_{26} \\ A_{16} & A_{16} & A_{66} & 0 & 0 & B_{16} & B_{26} & B_{66} \\ 0 & 0 & 0 & A_{44}^{(H)} & A_{45}^{(H)} & 0 & 0 & 0 \\ 0 & 0 & 0 & A_{45}^{(H)} & A_{55}^{(H)} & 0 & 0 & 0 \\ B_{11} & B_{12} & B_{16} & 0 & 0 & D_{11} & D_{12} & D_{16} \\ B_{12} & B_{22} & B_{26} & 0 & 0 & D_{12} & D_{22} & D_{26} \\ B_{16} & B_{26} & B_{66} & 0 & 0 & D_{16} & D_{26} & D_{66} \end{bmatrix} \begin{Bmatrix} \varepsilon_{xx} \\ \varepsilon_{ss} \\ \gamma_{xs} \\ \gamma_{sn} \\ \gamma_{xn} \\ \kappa_{xx} \\ \kappa_{ss} \\ \kappa_{xs} \end{Bmatrix}, \tag{B.3}$$

where N_{xx}, N_{ss}, and N_{xs} are axial, hoop and shear-membrane shell forces, respectively; N_{xn}, N_{sn} are transverse shear shell forces; and M_{xx}, M_{ss} and M_{xs} are axial and hoop bending and twisting shell moments, respectively; whereas ε_{xx} and ε_{ss} are axial and hoop normal shell strains, respectively; γ_{xs}, γ_{sn} and γ_{sn} are shear shell strains; κ_{xx}, κ_{ss} and κ_{xs} are axial, hoop and twisting curvatures, respectively. The coefficients A_{ij}, B_{ij}, D_{ij} and $A_{ij}^{(H)}$are shell stiffness-coefficients integrated in the thickness domain as defined in References [1,2]. Now, from expression (B.3) and neglecting hoop, thickness and inter-laminar shell-stress-resultants ($N_{ss} = N_{sn} = N_{xn} = M_{ss} = 0$) and rearranging the shell strains ε_{ss} and κ_{ss} in the remaining equations, it is possible to obtain the basic constitutive relations:

$$\begin{Bmatrix} N_{xx} \\ N_{xs} \\ M_{xx} \\ M_{xs} \end{Bmatrix} = \begin{bmatrix} \bar{A}_{11} & \bar{A}_{16} & \bar{B}_{11} & \bar{B}_{16} \\ & \bar{A}_{66} & \bar{B}_{16}^{*} & \bar{B}_{66} \\ & & \bar{D}_{11} & \bar{D}_{16} \\ & \text{sym} & & \bar{D}_{66} \end{bmatrix} \begin{Bmatrix} \varepsilon_{xx} \\ \gamma_{xs} \\ \kappa_{xx} \\ \kappa_{xs} \end{Bmatrix}, \tag{B.4}$$

where $\bar{A}_{ij}$ are the components of the reduced bending–extension coupling matrix, $\bar{B}_{ij}$ are components of the reduced bending–extension coupling matrix, $\bar{D}_{ij}$ are components of the reduced bending stiffness matrix. These coefficients are given by the following expressions:

$$\bar{A}_{11} = A_{11} + \frac{(2A_{12}B_{12}B_{22} - A_{22}B_{12}^2 - D_{22}A_{12}^2)}{A_{22}D_{22} - B_{22}^2},$$

$$\bar{A}_{16} = A_{16} + \frac{(A_{26}B_{12}B_{22} - A_{22}B_{12}B_{26} + A_{12}B_{26}B_{22} - A_{12}B_{26}D_{22})}{A_{22}D_{22} - B_{22}^2},$$

$$\bar{A}_{66} = A_{66} + \frac{(2A_{26}B_{26}B_{22} - A_{22}B_{26}^2 - D_{22}A_{26}^2)}{A_{22}D_{22} - B_{22}^2},$$

$$\bar{B}_{11} = B_{11} + \frac{(B_{12}B_{22}^2 - A_{22}B_{12}D_{12} + A_{12}B_{22}D_{12} - A_{12}D_{22}B_{12})}{A_{22}D_{22} - B_{22}^2},$$

$$\bar{B}_{16} = B_{16} + \frac{(B_{12}B_{22}B_{26} - A_{12}B_{26}D_{22} - A_{22}B_{12}D_{26} + A_{12}D_{26}B_{22})}{A_{22}D_{22} - B_{22}^2},$$

$$\bar{B}_{16}^{*} = B_{16} + \frac{(B_{12}B_{22}B_{26} - D_{12}B_{26}A_{22} - D_{22}B_{12}A_{26} + D_{12}A_{26}B_{22})}{A_{22}D_{22} - B_{22}^2},$$

$$\bar{B}_{66} = B_{66} + \frac{(B_{22}B_{26}^2 - A_{26}B_{26}D_{22} + A_{26}B_{22}D_{26} - A_{22}D_{26}B_{26})}{A_{22}D_{22} - B_{22}^2},$$

$$\bar{D}_{11} = D_{11} + \frac{(2B_{12}B_{22}D_{12} - A_{22}D_{12}^2 - D_{22}B_{12}^2)}{A_{22}D_{22} - B_{22}^2},$$

$$\bar{D}_{16} = D_{16} + \frac{(B_{26}B_{22}D_{12} - B_{12}B_{26}D_{22} + B_{12}B_{22}D_{26} - A_{22}B_{26}D_{12})}{A_{22}D_{22} - B_{22}^2},$$

$$\bar{D}_{66} = D_{66} + \frac{(2B_{26}B_{22}D_{26} - A_{22}D_{26}^2 - D_{22}B_{26}^2)}{A_{22}D_{22} - B_{22}^2}. \tag{B.5}$$

It is interesting to note that, although $\bar{B}_{16}$ and $\bar{B}_{16}^*$ have different algebraic forms; they have practically the same numerical value, even in the case of complex lamination sequence [14].

References

[1] E.J. Barbero, *Introduction to Composite Material Design*, Taylor & Francis Inc., Philadelphia, 1999.
[2] R.M. Jones, *Mechanics of Composite Materials*, Taylor & Francis Inc., Philadelphia, 1999.
[3] N.R. Bauld Jr., L.S. Tzeng, A Vlasov theory for fiber-reinforced beams with thin-walled open cross sections, *International Journal of Solids and Structures* 20 (3) (1984) 277–297.
[4] V. Giavotto, M. Borri, L. Mantegaza, G. Ghiringhelli, V. Carmaschi, C.G. Maffioli, F. Mussi, Anisotropic beam theory and applications, *Computers and Structures* 16 (1983) 403–413.
[5] O.A. Bauchau, A beam theory for anisotropic materials, *Journal of Applied Mechanics* 52 (2) (1985) 416–422.
[6] L.W. Rehfield, A.R. Atilgan, D.H. Hodges, Non-classical behavior of thin-walled composite beams with closed cross-sections, *Journal of American Helicopter Society* 35 (3) (1990) 42–50.
[7] L. Librescu, O. Song, On the aeroelastic tailoring of composite aircraft swept wings modeled as thin walled beam structures, *Composites Engineering* 2 (5–7) (1992) 497–512.
[8] O. Song, L. Librescu, Free vibration of anisotropic composite thin-walled beams of closed cross-section contour, *Journal of Sound and Vibration* 167 (1) (1993) 129–147.
[9] S. Na, L. Librescu, Dynamic response of elastically tailored adaptive cantilevers of non-uniform cross section exposed to blast pressure pulses, *International Journal of Impact Engineering* 25 (9) (2001) 847–867.
[10] V.H. Cortínez, M.T. Piovan, Vibration and buckling of composite thin-walled beams with shear deformability, *Journal of Sound and Vibration* 258 (4) (2002) 701–723.
[11] G.P. Dube, P.G. Dumir, Tapered thin open section beams on elastic foundation—II. Vibration analysis, *Computers and Structures* 61 (5) (1996) 897–908.
[12] S.R. Rao, N. Ganesan, Dynamic-response of tapered composite beams using higher-order shear deformation-theory, *Journal of Sound and Vibration* 187 (5) (1995) 737–756.
[13] L. Librescu, S. Na, Active vibration control of doubly tapered thin-walled beams using piezoelectric actuation, *Thin-walled Structures* 39 (1) (2001) 65–82.
[14] M.T. Piovan, Theoretical and Computational Study on the Mechanics of Thin-Walled Curved Beams made of Composite Materials considering Non-conventional Effects. PhD Dissertation, Universidad Nacional del Sur, Bahía Blanca, Argentina, 2003 (in Spanish).
[15] V.H. Cortínez, M.T. Piovan, Stability of composite thin-walled beams with shear deformability, *Computers and Structures* 84 (15–16) (2006) 978–990.
[16] M.T. Piovan, V.H. Cortínez, The transverse shear deformability in dynamics of thin walled composite beams: consistency of different approaches, *Journal of Sound and Vibration* 285 (3) (2005) 721–733.
[17] M.T. Piovan, V.H. Cortínez, Mechanics of shear deformable thin-walled beams made of composite materials, *Thin-Walled Structures* 45 (1) (2007) 37–72.
[18] C.P. Filipich, M.R. Escalante, M.B. Rosales, Power Series: an advantageous alternative applied to the free vibrations of frames, *Mecánica Computacional* 22 (2003) 908–920 (in Spanish).
[19] C.P. Filipich, M.B. Rosales, F.S. Buezas, Free vibration of symmetric arches of arbitrary guideline calculated by means of power series, *Mecánica Computacional* 22 (2003) 892–907 (in Spanish).
[20] M.B. Rosales, C.P. Filipich, Full modeling of the mooring non-linearity in a two-dimensional floating structure, *International Journal of Non-Linear Mechanics* 41 (2006) 1–17.